Efficient hydrologic tracer-test design for tracer-mass estimation and sample-collection frequency, 1. Method development

Malcolm S. Field

Abstract Hydrological tracer testing is the most reliable diagnostic technique available for the determination of basic hydraulic and geometric parameters necessary for establishing operative solute-transport processes. Tracer-test design can be difficult because of a lack of prior knowledge of the basic hydraulic and geometric parameters desired and the appropriate tracer mass to release. A new efficient hydrologic tracer-test design (EHTD) methodology has been developed to facilitate the design of tracer tests by root determination of the one-dimensional advection–dispersion equation (ADE) using a preset average tracer concentration which provides a theoretical basis for an estimate of necessary tracer mass. The method uses basic measured field parameters (e.g., discharge, distance, cross-sectional area) that are combined in functional relationships that describe solute-transport processes related to flow velocity and time of travel. These initial estimates for time of travel and velocity are then applied to a hypothetical continuous stirred tank reactor (CSTR) as an analog for the hydrological-flow system to develop initial estimates for tracer concentration, tracer mass, and axial dispersion. Application of the predicted tracer mass with the hydraulic and geometric parameters in the ADE allows for an approximation of initial sample-collection time and subsequent sample-collection frequency where a maximum of 65 samples were determined to be necessary for describing the predicted tracer-breakthrough curve (BTC). Inclusion of tracer retardation and decay cause a net increase in tracer-mass estimates so that the preset average tracer concentration will be maintained and there will be a consequent steepening of the BTC, but retardation also causes BTC spreading and a delay in tracer arrival.

Keywords Tracer-test design · Continuous stirred tank reactor · Breakthrough curves · Advection–dispersion equation · Functional relationships

Introduction

Tracer tests are regularly applied in many hydrological systems for determination of various hydraulic and geometric parameters. However, the success of a tracer test depends on the release of sufficient, but not excessive, tracer material into the flow regime for reliable tracer detection based on appropriate initial sample-collection time and sampling frequency. Determination of the optimal quantity of tracer material to release into a flow system to maximize the probability of achieving positive results while maintaining safe concentrations in the environment and minimizing public concern has been of considerable interest for a long time.

To maintain safe tracer concentrations and to minimize public concerns regarding colored water Field and others (1995) suggested that fluorescent-dye concentrations at downstream receptors be maintained at or below 1–2 mg L^{-1}. They arrived at 1–2 mg L^{-1} by conducting an in-depth evaluation of available toxicological information on 12 fluorescent dyes and one dye-intermediate utilizing an EPA-approved assessment method for cases where actual data were lacking. That paper urges the use of only that quantity of tracer dye actually needed to assure positive results. The use of significantly more than is needed might adversely affect the environment and human health although the degree of adversity was not quantified. In addition, excessive amounts of tracer could compromise tracer-test interpretations. However, determination of adequate and safe amounts of tracer substance, dye or otherwise, to use in a tracing study can be difficult to ascertain (Käss 1998, p. 327).

Disclaimer: The views expressed in this paper are solely those of the author and do not necessarily reflect the views or policies of the US Environmental Protection Agency.

Received: 9 January 2002 / Accepted: 1 April 2002
Published online: 12 June 2002

M.S. Field
US Environmental Protection Agency,
National Center for Environmental Assessment (8623D),
1200 Pennsylvania Ave NW, Washington, DC 20460, USA
E-mail: field.malcolm@epa.gov
Tel.: +1-202-5643279
Fax: +1-202-5650079

An optimal tracer mass to release that meets both hydrological and environmental criteria is dependent upon a number of relatively indeterminate factors, such as volume of water that dilutes the tracer, hydrological conditions during high-flow and low-flow periods, residence time, number and direction of discharge points, transport distance(s), sorption, decay, and degree and type of pollution. Therefore, the quantity of tracer needed for release at any particular site and time may be significantly different from that needed at another site or at the same site at another time.

For example, a preliminary tracer test at a Superfund site in Tennessee using 0.7 g of Rhodamine WT resulted in a conventional positively-skewed tracer-breakthrough curve (BTC) and nearly 100% mass recovery (Field and Pinsky 2000). A subsequent tracer test at the same site 48 h later using 71 g of Rhodamine WT produced a very abrupt BTC with a very long tail and only 28% mass recovery. A large storm that preceded the second tracer test was deemed responsible for the differing results (Field and Pinsky 2000).

To alleviate some of the difficulties associated with estimating the mass of tracer to be released, numerous empirical equations have been developed by various individuals (Field, unpublished). In nearly every instance these equations appear to have been devised without regard to solute-transport theory and at times, without regard to site hydrology. Rather, they appear to have been developed solely as a result of the developers' experience from one or more tracer tests. Also, in many instances various, and sometimes unexplained, multipliers are incorporated into the equations to account for potentially inadequate tracer-mass estimates (Field, unpublished).

Initial sample-collection times and sampling frequencies are also generally unknown quantities because solute fluxes are typically unknown. However, application of functional relationships developed from measured parameters can be used to estimate solute-transport parameters. Determinations of solute-transport parameters translate into appropriate sampling frequencies.

The purpose of this paper is to answer three basic questions common at the start of any hydrological tracer test: (1) how much tracer mass should be released, (2) when should sampling start, and (3) at what frequency should samples be collected? In this paper an efficient hydrologic tracer-test design (EHTD) methodology for estimating tracer mass based on solute-transport theory is developed. Use of the methodology developed here leads to a better understanding of the probable transport processes operating in the system prior to conducting the tracer test. Improved understanding of the transport processes then leads to better estimates of tracer mass to be released. In addition, initial sample-collection times and sample-collection frequencies are calculated using solute-transport theory. Part 2 of this series applies this methodology to several previously conducted tracer tests and compares the actual results to those predicted by this method without using the actual results to bias the predictions (Field 2002). Although this tracer-design methodology is expected to be reliable in most instances, it does not address the common occurrences of multimodal BTCs and long-tailed BTCs because such BTCs require much more complex analyses with numerous unknown parameters (Małoszewski and others 1992; Toride and others 1993). Density-induced sinking effects that may occur in natural gradient porous-media tracer tests (Oostrom and others 1992; Barth and others 2001) are also not addressed. The methodology introduced here is tracer independent while density-induced sinking is a tracer-dependent process and requires a separate analysis to determine what if any tracer sinking may occur.

Tracer-test design methodology

Previous efforts aimed at estimating tracer mass to be released for a tracer test focused primarily on expected dilution and drew upon the originators' experience. None of the previous efforts appear to have been derived according to solute-transport theory. It would also appear that solute-transport theory was seldom considered in designing tracer-sampling schedules. Solute-transport theory in natural and controlled systems has been investigated extensively and is well understood. It would seem appropriate then to consider solute-transport theory as a tool for determining the optimal tracer mass for release and sample-collection frequency.

Solute-transport modeling

Numerous model variations designed to describe solute transport have been developed. A general one-dimensional advection–dispersion equation (ADE) typically appears as (see Notations section)

$$R_d \frac{\partial C}{\partial t} = D_z \frac{\partial^2 C}{\partial z^2} - \upsilon \frac{\partial C}{\partial z} - \mu C \tag{1}$$

The retardation factor R_d can represent retardation in porous media by (Freeze and Cherry 1979, p. 404)

$$R_d = 1 + \frac{\rho_b K_d}{\theta} \tag{2a}$$

or R_d can represent retardation in fractured media by (Freeze and Cherry 1979, p. 411)

$$R_d = 1 + \frac{2K_a}{b} \tag{2b}$$

or R_d can represent retardation in a solution conduit by (Field and Pinsky 2000)

$$R_d = 1 + \frac{2K_a}{r} \tag{2c}$$

The first-order rate coefficient for tracer decay μ in porous media is given as (Toride and others 1995, p. 3)

$$\mu = \mu_l + \frac{\rho_b K_d \mu_s}{\theta} \tag{3a}$$

in fractured media may be taken as

$$\mu = \mu_l + \frac{2K_a\mu_s}{b} \tag{3b}$$

and in solution conduits may be taken as

$$\mu = \mu_l + \frac{2K_a\mu_s}{r} \tag{3c}$$

If tracer decay for the liquid phase μ_l equals tracer decay for the sorbed phase μ_s then the combined first-order decay μ is equal to $\mu_l R_d$ (Toride and others 1995, p. 4), which is a reasonable assumption commonly employed (Toride and others 1995, p. 35).

Tracer-mass estimation

The most straightforward method for estimating tracer mass is to obtain a solution to Eq. (1) and then solve for average concentration or its real root $f(x^*)\approx 0$. As a basic control, it is necessary to include a desired average concentration $\bar{C}$ that corresponds to average time $\bar{t}$ or peak concentration C_p that corresponds to peak time t_p.
A simple solution to Eq. (1) for a Dirac (δ) function for obtaining the maximum tracer concentration that ignores tracer retardation and decay is

$$f(x*) = C_p - \frac{M}{An_e\sqrt{4\pi D_z t_p}} \tag{4}$$

which may be solved explicitly for tracer mass M. Equation (4) will generally provide a reasonable estimate for M provided reasonable estimates are available for the other parameters. However, Eq. (4) may be oversimplified for many applications because it only deals with peak concentration and lacks consideration of tracer retardation and tracer decay. Applying Eq. (4) may result in excessive tracer-mass estimates, which is neither desirable from a hydrological, aesthetic, economical, human health, or ecological perspective, nor necessary to achieve positive tracer recovery. Alternatively, actual tracer retardation and/or tracer decay may result in tracer-mass estimates that are too small for adequate tracer recovery.
Application of more comprehensive solutions to Eq. (1) will provide a more reasonable and reliable estimate for tracer mass to be injected. Some solutions to Eq. (1) can be evaluated explicitly for M, but other solutions for Eq. (1) may require evaluation for its real root for some $x^*\in[a_1,a_2]$ where x^* represents the estimated mass M.

Model solutions

Solutions for Eq. (1) for impulse and pulse releases are most appropriate for estimating tracer mass. A continuous release is less relevant because most tracer tests involve a finite time period for release. Although not a physical reality, it is probable that most tracer tests, especially in karstic aquifers, attempt to achieve an impulse release that may be described as a Dirac (δ) pulse. However, many attempts at an impulse release are actually pulse releases due to the time involved for the tracer to reach the flow system under investigation (Field 1997; Field and Pinsky 2000).

Impulse release

Applying the dimensionless parameters listed in the Notations section to Eq. (1) results in (Toride and others 1995, p. 4)

$$R_d\frac{\partial C_f}{\partial T} = \frac{1}{P_e}\frac{\partial^2 C_f}{\partial Z^2} - \frac{\partial C_f}{\partial Z} - \mu^E C_f \tag{5}$$

which when solved for the boundary value problem is (modified from Toride and others 1995, p. 13)

$$f(x*) = \bar{C}^E(Z,\ \bar{T}) - M_B\Gamma_1^E(Z,\ \bar{T}) \tag{6}$$

where $\bar{C}^E(Z,\ \bar{T})$ is a preset mean volume-averaged concentration that corresponds to dimensionless distance Z and dimensionless mean residence time $\bar{T}$. The auxiliary function Γ_1^E is defined in Table 1.
Solving Eq. (6) explicitly for M or for its real root as it relates to $\bar{C}^E(Z,\ \bar{T})$ limits the solution to the concentration corresponding with average travel time which will be less than the peak concentration.

Pulse release

The solution to Eq. (5) for a pulse release for the case where $\mu^E=0$ is (modified from Toride and others 1995, p. 14)

$$f(x*) = \bar{C}^E(Z,\ \bar{T}) - \sum_{i=1}^{2}(g_i - g_{i-1})\Gamma_2^E\left(Z,\ \bar{T} - \hat{T}_i\right) \tag{7}$$

and for the case where $\mu^E \neq 0$ is (modified from Toride and others 1995, p. 14)

$$f(x*) = \bar{C}^E(Z,\ \bar{T}) - \sum_{i=1}^{2}(g_i - g_{i-1})\Gamma_3^E\left(Z,\ \bar{T} - \hat{T}_i\right) \tag{8}$$

where Eqs. (7) and (8) are again solved for the real root as related to $\bar{C}^E(Z,\ \bar{T})$ in which the result will be less than the peak concentration. The auxiliary functions Γ_2^E and Γ_3^E are defined in Table 1.

Table 1
Expressions for Γ^E in the solutions for flux-averaged concentrations (Toride and others 1993, 1995, pp. 13–14)

Function	Flux-averaged concentration, C_f
Γ_1^E	$e^{-\mu^E\bar{T}/R_d}\sqrt{\frac{R_d P_e Z}{4\pi\bar{T}^3}}e^{-P_e(R_dZ-\bar{T})^2/4R_d\bar{T}}$
Γ_2^E	$\frac{1}{2}\,erfc\left(\frac{R_dZ-\bar{T}}{\sqrt{4R_d\bar{T}/P_e}}\right) + \frac{1}{2}\,e^{PeZ}erfc\left(\frac{R_dZ+\bar{T}}{\sqrt{4R_d\bar{T}/P_e}}\right)$
Γ_3^E	$\frac{1}{2}\,e^{P_e(1-u)Z/2}erfc\left(\frac{R_dZ-u\bar{T}}{\sqrt{4R_d\bar{T}/P_e}}\right) + \frac{1}{2}\,e^{P_e(1+u)Z}erfc\left(\frac{R_dZ+u\bar{T}}{\sqrt{4R_d\bar{T}/P_e}}\right)$
	$u = \sqrt{1+\frac{4\mu^E}{P_e}},\ \left(\mu^E > \frac{-P_e}{4}\right)$

Tracer retardation and tracer decay

Application of any solution to Eqs. (1) or (5) for instances where tracer retardation and tracer decay are significant (R_d>1; μ>0) can have profound effects on the shape of the BTC. Commonly, increasing R_d tends to cause a flattening, lengthening, and spreading of the BTC, while increasing μ only causes a flattening of the BTC.

Conversely, increasing R_d when using Eqs. (6), (7), or (8) results in a steepening, lengthening, and spreading of the BTC. An increase in R_d has the effect of reducing the calculated value for $\bar{C}^E$, which causes a concomitant increase in estimated mass M so that the set value for $\bar{C}^E$ can be maintained. A lengthening and spreading of the BTC continue in a normal manner because the time of travel t is not considered in the root determination.

Increasing μ when solving for the root also causes a steepening of the BTC because it also has the effect of reducing the calculated value for $\bar{C}^E$. The net effect is to cause an increase in estimated mass M so that the preset value for $\bar{C}^E$ can be maintained.

Solute transport

Preliminary estimates for tracer mass in conjunction with travel time estimates and related hydraulic parameters may be applied to any particular solution to Eq. (5) to obtain a BTC. Inverse analysis using the estimated parameters M, R_d, and/or μ and the predicted BTC can be conducted to observe the sensitivity of the model to any one of the three parameters.

The primary difficulty with application of any particular solution to the ADE is the need to estimate not only the tracer mass, but the times of travel ($\bar{t}$, t_p, and t_i), which are related to flow velocity (υ, υ_p, υ_i) and axial dispersion D_z. An inability on the part of the originators of previous tracer-mass estimation equations (Field, unpublished) to estimate $\bar{t}$, υ, and D_z prior to initiating a tracer test is the most likely reason why solute-transport theory was ignored when developing tracer-mass estimation methods. Because $\bar{t}$ and D_z can take on a wide range even when assuming steady-flow conditions, reasonable initial estimates for $\bar{t}$ and D_z can be difficult to obtain and are most commonly acquired from a tracer test.

Estimates for hydraulic parameters can, however, be obtained from some basic flow-system measurements, functional relationships, and consideration of a simple conceptual model of the flow system. Although the simple model and functional relationships may only be approximations, they are likely to be sufficiently reliable as to lead to a good approximation of some basic hydraulic parameters necessary for a successful tracer test.

Hydraulic and geometric parameters

Use of Eqs. (6), (7), or (8) for assessing transport processes and predicting tracer mass requires specific hydraulic and geometric parameters measured in the field be combined in simple functional relationships. These measured parameters and functional relationships can then be applied in a simple hypothetical model as a precursor to application of the ADE.

Measured parameters

For flowing streams in surface channels or solution conduits, measurements for discharge Q, cross-sectional area A, and transport distance L need to be taken. These three parameters are the most important measurable field parameters necessary for establishing basic hydraulic and geometric controls in any hydrologic system.

For porous media, additional measurements or estimates for specific parameters must also be taken. These additional parameters are expected transverse spread W and vertical spread H of the tracer plume and effective porosity n_e. Moreover, it is necessary that the type of tracer test be identified as either a natural-gradient test or a forced-gradient tracer test in which a radially symmetric flow field is created by an extraction well.

Functional relationships

Discharge, cross-sectional area, and transport distance can each be measured at a downstream location such as a spring for a karst aquifer or estimated from Darcy's law for a porous-media aquifer. Transport distance in solution conduits may be corrected for sinuosity by multiplying by a sinuosity factor ≤ 1.5 (Sweeting 1973, p. 231). Surface stream or solution conduit volume V may be estimated by

$$V = AL \tag{9}$$

Aquifer volume for porous media with regional gradient is estimated by

$$V = LWH \tag{10}$$

and aquifer volume for porous media under forced-gradient conditions is estimated by

$$V = \pi L\left(\frac{H}{2}\right)^2 \tag{11}$$

Average flow velocity υ for a surface stream or solution conduit may be estimated from

$$\upsilon = \frac{Q}{A} \tag{12}$$

or, for a natural-gradient tracer test in porous media, by application of Darcy's law. Initial average flow velocity for a natural-gradient tracer test will conform to the basic form of Eq. (12) when n_e is included

$$\upsilon = \frac{Q}{WHn_e} \tag{13}$$

although the width W may be difficult to estimate. If W cannot reasonably be estimated, then velocity is estimated from

$$\upsilon = \frac{Q}{LHn_e} \tag{14}$$

which is not theoretically correct, but may result in an acceptable approximation.
For a forced-gradient tracer test in porous media in which the gradient is influenced by either a single extraction well or by a combination of an injection well and a withdrawal well, velocity may be estimated from (Käss 1998, p. 377)

$$\upsilon = \frac{Q}{\pi LHn_e} \tag{15}$$

and for an injection-withdrawal tracer test with recirculation from (Webster and others 1970)

$$\upsilon = \frac{3Q}{\pi LHn_e} \tag{16}$$

Travel time estimates

Estimates for transport velocities translate directly into transport times. Initial average time of travel $\bar{t}$ is estimated from

$$\bar{t} = \frac{L}{\upsilon} \tag{17}$$

and tracer-test duration from

$$t_d = \frac{n_m L}{\upsilon} \tag{18}$$

where $2 \le n_m \le 3$ depending on the type of tracer release. Parriaux and others (1988, p. 8) recommend n_m=3, but it was experimentally established that setting n_m=2 for impulse releases and n_m=3 for pulse releases produces the best results.
Individual tracer travel time data points must also be estimated. A base time value t_b for initial time t_1 and subsequent time spacing Δt may be estimated up to $\bar{t}$ by

$$t_b = \frac{n_m \bar{t}}{n} \tag{19}$$

and a base time value t_m for subsequent time spacing $n_m \Delta t$ from $\bar{t}$ may be estimated by

$$t_m = n_m t_b \tag{20}$$

By assuming $\bar{t}=t_p$ individual time values t_i may be calculated up to $\bar{t}$ from

$$t_i = t_b + \sum_{i=1}^{n/2} t_{n_i} \tag{21}$$

and individual time values t_i from $\bar{t}$ from

$$t_i = t_m + \sum_{i=n/2}^{n} t_{n_i} \tag{22}$$

where n is a reasonable number of data points appropriate for obtaining a smooth BTC. Combining the values obtained from Eqs. (21) and (22) results in a series of appropriately spaced time values that approximates initial tracer arrival and final tracer detection. Doubling or tripling time spacing after $\bar{t}$ is not really necessary. However, it is essential that sufficiently early and late times be established to ensure adequate consideration of actual flow conditions.

Continuous stirred tank reactor

Obtaining an estimate for M and D_z can be achieved for a predicted BTC based on the theory of a completely mixed continuous stirred tank reactor (CSTR). A mass-balance model that describes the dynamics of a simplified CSTR is (Silebi and Schiesser 1992, pp. 49–50)

$$\frac{d(VC)}{dt} = qC_0 - QC - VkC \tag{23}$$

Setting q=Q and using initial condition

$$C(0) = C_p \tag{24}$$

the solution to Eq. (23) is (Silebi and Schiesser 1992, p. 50)

$$C(t) = C_p e^{[-(Q+Vk)t/V]} \tag{25}$$

Equation (25) will produce an exponentially decaying BTC starting at the peak concentration C_p with a gradient that is dependent on the value of the reaction rate constant k and the space velocity Q/V (Levenspiel 1999, p. 93). It is apparent from Eq. (25) that whereas C_p may be preset, prior knowledge of discharge Q, reactor volume V, and transport times t must be determined.
Equation (25) is evaluated for C from $\bar{t} \approx t_p$ in a descending manner using $0.25 \le k \le 1.0$ although k=0 would adequately suffice. The concentration values C obtained from Eq. (25) leading from $\bar{t}$ are then reversed to achieve an ascending limb leading to $\bar{t}$. Equation (25) is then resolved for C from $\bar{t}$ in a descending manner using a k<<1.0. For n=200, k=1/200 represents a reasonable exponential decay for the descending limb.
The values for k were empirically determined such that $0.25 \le k \le 1.0$ represents a steeply ascending limb while k<<1.0 represents a more-gently decaying descending limb controlled by the number of data points. The result is a good approximation of a typically positively skewed BTC in which a cusp forms the peak concentration at the peak time of arrival. Although the values for k were empirically determined, the resulting BTC appears to reasonably represent a typical BTC based on observation and experience.
The BTC produced by the CSTR model is subsequently evaluated by

$$M = Q \int_0^{\infty} C(t)dt \tag{26}$$

to obtain the area under the BTC. The area represents an initial estimate for the tracer mass to be adjusted as required by Eqs. (6), (7), or (8).

Travel times and velocity

For the purpose of determining axial dispersion D_z, tracer travel time weighted for tracer mass for impulse and short-pulse releases is estimated from

$$\bar{t} = \frac{\int_0^\infty tC(t)dt}{\int_0^\infty C(t)dt} \tag{27}$$

and tracer travel time variance $\sigma^2{}_t$ is estimated from

$$\sigma_t^2 = \frac{\int_0^\infty (t-\bar{t})^2 C(t)dt}{\int_0^\infty C(t)dt} \tag{28}$$

where C is obtained from Eq. (25). The CSTR-generated BTC is predicated on the assumption of an impulse or short-pulse release so other forms of Eqs. (27) and (28) are not required.

In the same manner, a mean velocity $\bar{\upsilon}$ is obtained for use in estimating axial dispersion by the method of moments. For an impulse release $\bar{\upsilon}$ is obtained from

$$\bar{\upsilon} = \frac{\int_0^\infty \frac{z}{t} C(t)dt}{\int_0^\infty C(t)dt} \tag{29a}$$

and for a pulse release $\bar{\upsilon}$ is obtained from

$$\bar{\upsilon} = \frac{\int_0^\infty \frac{z}{t-t_0/2} C(t)dt}{\int_0^\infty C(t)dt} \tag{29b}$$

where $\bar{\upsilon} \le \upsilon$.

Tracer dispersion estimates

Axial dispersion may be determined using the method of moments theory. Although statistically and theoretically valid the method of moments has the tendency to overestimate dispersion. Alternatively, the effects of velocity variations, matrix diffusion and immobile-flow regions can create the appearance of significant dispersion. These difficulties require that dispersion estimates be obtained in a manner that considers the method of moments, while reducing the influence of long tails. This is most easily accomplished using the Chatwin method (Chatwin 1971) in conjunction with the method of moments.

Estimating dispersion by the method of moments

Axial dispersion properly weighted for concentration may be estimated for an impulse release by

$$D_z = \frac{\sigma_t^2 \bar{\upsilon}^3}{2z} \tag{30}$$

and for a short-pulse release by (Wolff and others 1979)

$$D_z = \left(\sigma_t^2 - \frac{t_0}{12}\right)\frac{\bar{\upsilon}^3}{2z} \tag{31}$$

It should be recognized here that D_z solved by Eq. (31) is based on the assumption of a BTC and does not represent the mean residence time distribution as does Eq. (30). There will usually not be any major difference in D_z estimation from Eqs. (30) or (31). In addition, because the CSTR-generated BTC is based on an impulse release Eq. (31) may reasonably be ignored even though the subsequent tracer test may be a pulse or step test.

Estimating dispersion by the Chatwin method

Axial dispersion may be estimated using a modification of the method developed by Chatwin (1971) given by

$$\sqrt{t_i \ln\left(\frac{C_p\sqrt{t_p}}{C_i\sqrt{t_i}}\right)} = \frac{z}{2\sqrt{D_z}} - \frac{\upsilon t_i}{2\sqrt{D_z}} \tag{32}$$

Subject to $t_\kappa \le z/\upsilon$, Eq. (32) is reduced to the general least-squares problem by solving

$$\min_x \|\mathbf{b} - \mathbf{A}\mathbf{x}\|_2^2 \tag{33}$$

where

$$\mathbf{A} = \begin{pmatrix} 1 & t_1 \\ 1 & t_2 \\ \vdots & \vdots \\ 1 & t_\kappa \end{pmatrix} \tag{34}$$

$$\mathbf{x} = (x_1,\ x_2)^T \tag{35}$$

$$\mathbf{b} = (b_1,\ b_2,\ \ldots,\ b_\kappa)^T \tag{36}$$

The parameters b_i are equal to the left-hand side of Eq. (32)

$$b_i = \sqrt{t_i \ln\left(\frac{C_p\sqrt{t_p}}{C_i\sqrt{t_i}}\right)} \tag{37}$$

and the parameters to be determined x_i are equal to the two factors on the right-hand side of Eq. (32)

$$x_1 = \frac{z}{2\sqrt{D_z}} \tag{38}$$

$$x_2 = \frac{\upsilon}{2\sqrt{D_z}} \tag{39}$$

where x_1 is the y intercept of the straight-line fit to the early-time data and x_2 is the gradient of the straight-line fit to the early-time data.

Equations (30) and (31) tend to overestimate D_z for nonporous-medium flow systems, which will generally result in an overestimation of estimated tracer mass needed and a greater BTC spread than is likely to occur as a result of solute dispersion. Alternatively, Eq. (32) tends to underestimate D_z for porous-medium flow systems, which will have an effect opposite that of Eqs. (30) and (31).

For these two reasons, Eq. (32) is used to estimate D_z for a nonporous-medium flow system while Eq. (30) and/or Eq. (31) are used to estimate D_z for porous-medium flow

systems. Although not precise measures of D_z, these estimates for D_z are believed to be adequate for the purpose of obtaining an approximation of D_z for use in Eqs. (6), (7), or (8).

Tracer sample-collection design

Solute-transport parameter estimates are used in Eqs. (6), (7), or (8) with the initial estimate for tracer mass. Adjustments to the initial estimate for tracer mass are made iteratively based on the estimated solute-transport parameters, preset mean volume-averaged concentration $\bar{C}^E$, and any effects created by suggested tracer reactions. Final estimates are then used in the ADE to generate a BTC representative of the flow system to be traced.

Sample collection

The ADE-generated BTC serves as the basis for determining an appropriate sampling frequency and a determination for initial sample-collection time. Rather than using conjecture, transport distance, or unmeasured estimates for tracer velocity as is common (Field, unpublished), the BTC allows for realistic consideration of the times of travel.

Sampling frequency

Sample-collection frequency is based on an arbitrary number of samples to be collected that balances the cost of sample collection and analysis with the value of an ever increasing number of samples. An adequate sampling frequency necessary for representing a continuous series by a discrete series must be determined for the extraction of optimal information while maximizing the accuracy of the results and minimizing the computational costs. The sampling frequency then is based on how rapidly tracer concentration is changing so that as the average $|dC/dt|$ increases, sampling frequency should also increase (Yevjevich 1972, p. 2).

The number of samples n_s to be collected can be arbitrarily chosen initially. Novakowski (1992) has suggested that n_s equal at least 20–30 samples with the greatest concentration of samples occurring around C_p, which assumes that C_p is known, whereas Kilpatrick and Wilson (1989, p. 18) suggest n_s=30 samples will generally be necessary as a minimum for defining the BTC. To properly define rapid changes in the BTC, n_s=60 was experimentally found to be more reliable if aliasing effects are to be avoided (Smart 1988). Aliasing of a multimodal BTC is a common problem when an inadequate sampling frequency is applied to a tracer test exhibiting complex behavior.

Sampling frequency may then be determined from

$$t_{sf} = \frac{t_d - t_{sm}}{n_s} \tag{40}$$

where t_{sm} corresponds to the first instance that $C_i > 10^{-3}\ C_p$ μ g/L. These values for t_{sm} are used on the assumption that lower concentrations are not readily detectable nor necessarily relevant.

Initial sample collection

Once the sampling frequency has been determined the initial sample-collection time is adjusted backwards by an additional number of selected samples n_b. Initial sample-collection time t_{s1} is then obtained by subtracting t_{sf} from t_{sm} for a selected number of additional samples n_b. For most instances n_b=5 may be taken as a reasonable number of additional samples to collect prior to the occurrence of $t_{s1}=t_{sm}$. All subsequent sampling times are found from

$$t_{si} = t_{sf} + \sum_{i=1}^{n_s} t_{s_i} \tag{41}$$

The total number of samples to be collected with an associated sampling time spacing t_{sf} can be subsequently divided into fractions thereof as desired. Earlier sample collection than the recommended t_{s1} may be considered as appropriate. Sample collection ending times other than t_d may also be determined depending on whether tracer detection has ceased prior to reaching t_d or is continuing beyond t_d.

Methodology evaluation

Application of this tracer estimation methodology provides for a general sense of the appropriate tracer mass to release and general hydraulics of the system to be traced. Because the hydraulics of the system are approximated, sampling frequency and initial sample-collection time may also be predicted. The computer code, EHTD, facilitates the tracer-design methodology for typical hydrological settings using measured hydrological field parameters to calculate functional relationships. The measured parameters and functional relationships are then applied to a hypothetical CSTR to develop a preliminary BTC, which is then numerically evaluated by the method of moments for tracer mass and hydraulic parameter estimation. The calculated hydraulic parameters are then used in solving for estimated tracer mass and sampling times.

The CSTR-generated BTC is solved by the method of moments by developing a piecewise cubic Hermite function. That is, the interpolant is defined in terms of a set of cubic polynomials, each of which is defined between a pair of consecutive data points. The coefficients of these cubic polynomials are chosen so that the interpolant has continuous first derivatives and the remaining freedom of choice is used to ensure that the interpolant is visually acceptable, meaning that monotonicity in the data results in monotonicity in the interpolant which is defined by (Kahaner and others 1989, pp. 100–103 and 106–108)

$$g(t) \equiv \hbar(t) = \sum_{i=1}^{n} C_i \hbar_i(t) + d_i \hat{\hbar}_i(t) \tag{42}$$

A piecewise cubic Hermite function in effect produces the most reasonable interpolation of the data possible with

excellent theoretical convergence properties. Integration is then accomplished by cubic Hermite quadrature as (Kahaner and others 1989, pp. 161–162)

$$I \approx I\prime = \int_{t_1}^{t_d} \hbar(t)dt = \sum_{i=1}^{n} C_i \int_{t_1}^{t_d} \hbar_i(t) + d_i \int_{t_1}^{t_d} \hat{\hbar}_i(t) \quad (43)$$

which is the compound trapezoid rule with appropriate end corrections. The compound trapezoid rule is exceptionally accurate when the integrand is a smooth periodic function given by equally spaced data points (Kahaner and others 1989, p. 162).

Equations (6), (7), and (8) may be solved directly or by using a combination of the bisection method and the secant method. The bisection method ensures certainty while the secant method ensures rapid convergence. This combination of bisection and secant methods is very efficient, accurate, and guaranteed to produce reasonable results (Kahaner and others 1989, pp. 248–250).

For instances where tracer mass is expected to be adversely affected by retardation or decay, EHTD employs a constrained nonlinear least-squares optimization routine to adjust the tracer mass, retardation, and decay estimates relative to the BTC produced by the hypothetical CSTR. The nonlinear optimization routine searches for a vector $\mathbf{y}$ of p components that minimizes the sum of the squares function $f(y) = \frac{1}{2}\sum_{i=1}^{n} \hat{r}_i(y)^2$ that is constrained by $\underline{\gamma}_i \le y_i \le \bar{\gamma}_i$, $1 \le i \le p$ where the $\hat{r}_i(y)$ are twice continuously differentiable functions of y (Dennis and others 1981).

Simulation

The methodology described was tested using measured field parameters and functional relationships listed in Table 2 for Prospect Hill Spring located in Clarke County, Virginia. Figure 1 is a plot of time versus concentration produced by a hypothetical CSTR using the measured field parameters and functional relationships listed in Table 2. Integrating Fig. 1 produced a preliminary estimate for tracer mass, M=188 g. Of particular significance are the variable effects created by the measured field parameters when combined in functional relationships. Increasing Q, decreasing A, or decreasing L all have the effect of shifting the curve to the left and decreasing the mass estimate. Decreasing Q, increasing A, or increasing L all have the effect of shifting the curve to the right and increasing the mass estimate. Figure 2 is a plot of time versus concentration produced by the ADE using the measured field parameters and functional

Table 2
Tracer-test design parameters

Parameter	Value
Measured parameters	
Release mode	Impulse
Q, $m^3\ h^{-1}$	3.63×10^{2}
z[a], m	2.74×10^{3}
A, m^2	2.23×10^{0}
$\bar{C}^E$, $\mu g\ L^{-1}$	5.00×10^{1}
Functional relationships	
t_p, h	1.64×10^{1}
$\bar{t}$, h	1.69×10^{1}
υ_p, $m\ h^{-1}$	1.68×10^{2}
υ, $m\ h^{-1}$	1.63×10^{2}
V, m^3	6.12×10^{3}
Axial dispersion	
D_z, $m^2\ h^{-1}$	4.98×10^{3}
P_e	8.96×10^{1}
Tracer reaction	
R_d	1.00×10^{0}
μ, h^{-1}	0.00×10^{0}

[a]Transport distance = straight-line distance, 1.83×10^{3} m×sinuosity factor, 1.5

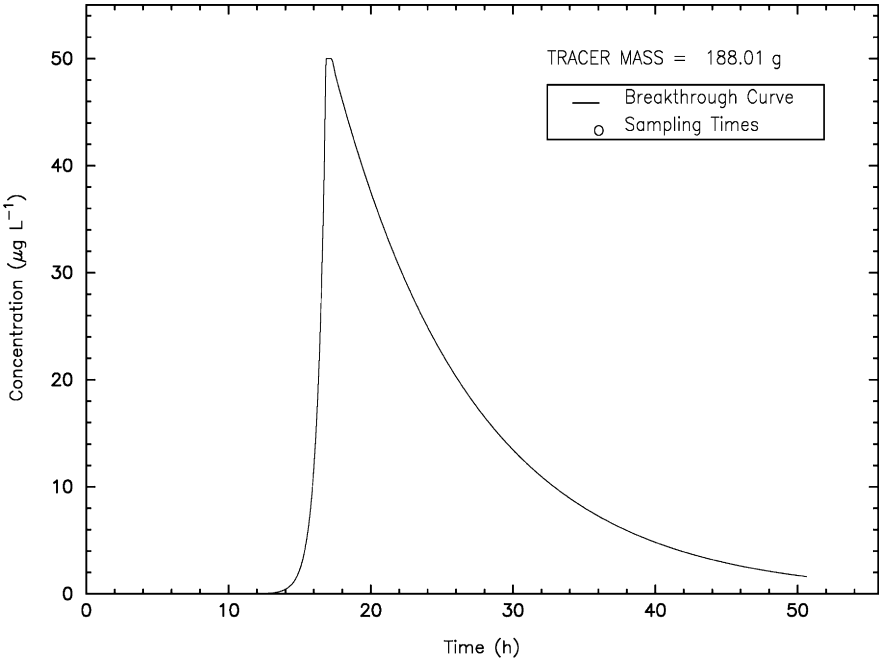

Fig. 1
Preliminary BTC generated from a hypothetical CSTR

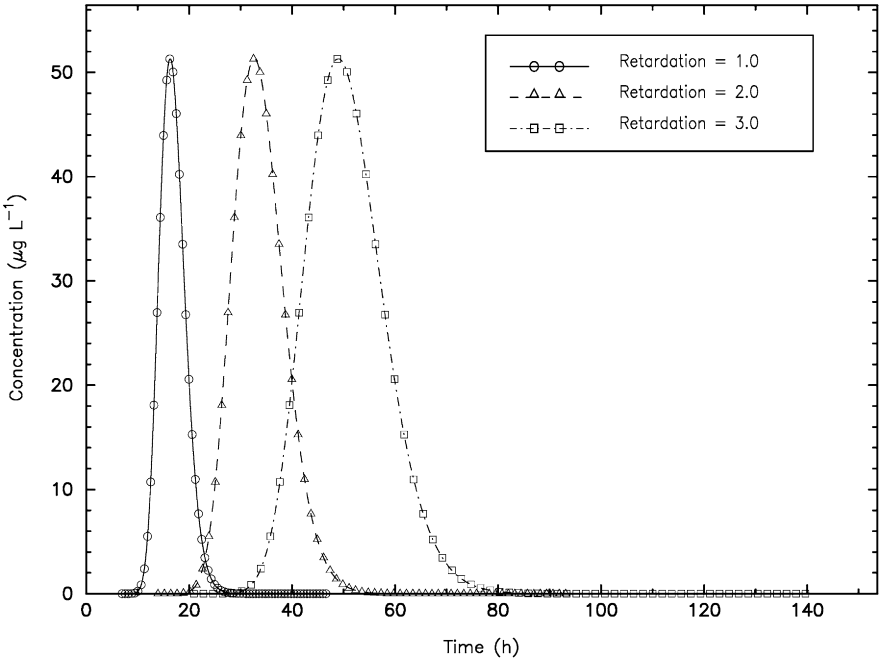

Fig. 2
Predicted BTC for Prospect Hill Spring for increasing values for retardation. *Symbols* represent recommended sampling times

relationships listed in Table 2 with varying tracer retardation (R_d=1, R_d=2, R_d=3) and no tracer decay (μ=0 h^{-1}). The predicted tracer mass necessary for a successful tracer test and resulting average and peak tracer concentrations are shown in Table 3 for varying tracer-reaction conditions. From Fig. 2 and Table 3 it is apparent that while $\bar{C}^E$ remains the same for each BTC for varying values of R_d, the $\bar{t}$ and D_z appear to increase and υ to decrease as R_d increases. In fact, these hydrologic parameters have not physically changed, but increasing R_d creates just such an appearance.

Table 3 also includes four instances of tracer decay (μ>0 h^{-1}) without retardation (R_d=1.0), the effects of which are shown in Fig. 3 for three of the instances (μ=0.0 h^{-1}, μ=0.05 h^{-1}, μ=0.1 h^{-1}), because μ=0.01 h^{-1} would not be readily distinguishable from μ=0.0 h^{-1}. Obvious from Fig. 3 is that as tracer decay is allowed to increase, C_p also increases (Table 3) because of the necessity of maintaining $\bar{C}^E$. This effect was not observed for increasing tracer retardation. In addition, because C_p increases, the BTC is steepened causing an apparent decrease in tracer transport times. However, whereas t_p clearly decreases (Fig. 3), $\bar{t}$ remains unchanged regardless of the proposed tracer reactions.

Increasing tracer-reaction effects causes a concomitant increase in tracer-mass estimates. The increase in tracer-mass estimates reflects the need to match the set value for $\bar{C}^E$ while including factors that have the net effect of decreasing tracer-mass estimates so that the overall effect is an estimate for tracer mass that approximates that which should be used in a tracer test.

Included on Figs. 2 and 3 is an indication of appropriate sampling times for each BTC (Table 4). Sixty-five sampling times were developed to adequately determine when the first sample should be collected and to properly define the BTC. Breakthrough curve definition requires that the BTC peak be correctly identified and that a potentially long tail be detected. Further, in order to avoid the effects of data aliasing, a substantial number of samples are required (Smart 1988). Although 20–30 samples have been suggested by others as adequate for BTC definition (Kilpatrick and Wilson 1989, p. 18; Novakowski 1992) these researchers were not concerned with problems associated with long tails or data aliasing. To ensure that data aliasing be avoided, 60 sample-collection times are developed by EHTD because it allows for better BTC definition while not requiring excessive sampling. However, should 60 samples prove to be excessive it is always possible to choose to

Table 3
Predicted tracer mass and tracer concentration

Tracer reaction			M, g	$\bar{C}^E$, μg L^{-1}	C_p, μg L^{-1}
R_d	K_a^a, m	μ, h^{-1}			
1.0	0.0	0.0	114.61	50.00	51.31
1.0	0.0	0.01	135.68	50.00	51.60
1.0	0.0	0.05	266.45	50.00	53.15
1.0	0.0	0.1	619.45	50.00	55.80
2.0	0.42	0.0	229.23	50.00	51.31
3.0	0.84	0.0	343.84	50.00	51.31

[a]K_a obtained for an assumed cylindrical solution conduit using Eqs. (2c) and (9)

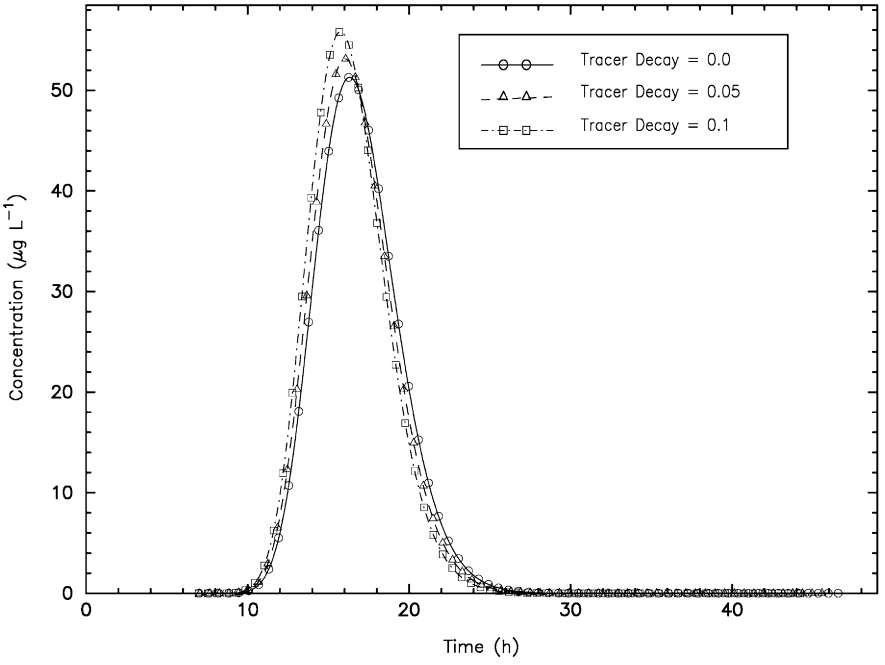

Fig. 3
Predicted BTC for Prospect Hill Spring for increasing values for tracer decay. *Symbols* represent recommended sampling times

Table 4
Recommended sampling times for selected tracer reaction conditions

Sample number	Sampling time, h					
	R_d^a=1.0 μ=0.0	R_d^b=1.0 μ=0.01	R_d^c=1.0 μ=0.05	R_d^d=1.0 μ=0.1	R_d^e=2.0 μ=0.0	R_d^f=3.0 μ=0.0
1	6.97	7.00	7.04	6.95	13.95	20.92
2	7.59	7.61	7.64	7.53	15.19	22.78
3	8.21	8.22	8.25	8.12	16.42	24.63
⋮	⋮	⋮	⋮	⋮	⋮	⋮
15	15.64	15.58	15.47	15.10	31.27	46.91
16[g]	16.25	16.19	16.07	15.68	32.51	48.76
17	16.87	16.81	16.67	16.27	33.75	50.62
⋮	⋮	⋮	⋮	⋮	⋮	⋮
63	45.33	45.01	44.35	43.04	90.66	132.28
64	45.95	45.62	44.95	43.62	91.90	137.85
65	46.57	46.23	45.56	44.21	93.14	139.70

[a]Recommended sampling frequency = 37.12 min
[b]Recommended sampling frequency = 36.78 min
[c]Recommended sampling frequency = 36.11 min
[d]Recommended sampling frequency = 34.93 min
[e]Recommended sampling frequency = 1.24 h
[f]Recommended sampling frequency = 1.86 h
[g]Approximate sampling time for peak concentration

collect some fraction of 60. To ensure that initial tracer breakthrough is not missed n_b=5 was included as an appropriate number of samples to collect prior to expected tracer breakthrough.

Conclusions

Hydrological tracer testing is an essential method of study for evaluating solute-transport processes. However, the initial design of most tracer tests can be problematic due to a lack of prior knowledge concerning the hydrological-transport properties for which the tracer test is intended. A simple reliable method for designing tracer tests has been developed by solving the one-dimensional ADE for a preset average tracer concentration. This tracer-design method provides a sound theoretical basis for estimating tracer mass and sample-collection frequency by combining basic field measurements for hydraulic and geometric parameters in functional relationships that describe solute-transport processes to estimate flow velocity and times of travel. These relationships are then applied to a hypothetical CSTR as an analog for the hydrological-flow system to develop estimates for tracer concentration and axial dispersion based on the preset average tracer concentration. Solution of the one-dimensional ADE using the preset average tracer concentration then allows for an

estimate of necessary tracer mass. Application of the predicted tracer mass with the hydraulic and geometric parameters in the ADE further allows for an approximation of initial sample-collection time and subsequent sample-collection frequency.

Tracer retardation and decay cause an increase in tracer-mass estimates because the set average tracer concentration is maintained by the method. Retardation has the added effect of delaying tracer breakthrough and causing more spread in the BTC, which can have significant consequences for determining when to initiate sample collection and at what frequency all subsequent samples should be collected. Experience with common tracers in various environments serves to trivialize this problem, however. Prior evaluations of distribution coefficients and simulations using selected values for retardation and decay can further limit the errors that may occur from tracer reactions with solids.

The method does not attempt to physically predict the conditions that may cause multimodal or long-tailed BTCs because it is not possible nor necessary to add such complexity. It also does not address the possible occurrence of density-induced sinking. Not only would estimates for unknown parameters be required (e.g., mass-transfer coefficient), the effect of adding such complexity would not greatly improve the estimates for required tracer mass or recommended sampling frequency.

Acknowledgements The author would like to thank Arthur Palmer of the State University of New York, and Dirk Young of the US Environmental Protection Agency for their careful review of the manuscript. Their helpful comments and suggestions greatly improved the manuscript and are gratefully acknowledged.

Notations

A	cross-sectional area of flow system (L^2)
$\mathbf{A}$	matrix of time values used in the Chatwin analysis (T)
a_i	interval of data points that bracket the function $f(x^*)$; (i=1,2)
b	one half fracture width (L)
b_κ	maximum allowable Chatwin parameter corresponding to t_κ ($T^{1/2}$)
$\mathbf{b}$	vector of concentration parameters for the Chatwin analysis ($T^{1/2}$)
C	tracer concentration (M L^{-3})
$\bar{C}$	average tracer concentration (M L^{-3})
$\bar{C}^E$	mean volume-averaged tracer concentration (M L^{-3})
C_f	dimensionless flux-average tracer concentration $= \frac{C}{c_0}$
c_0	characteristic tracer concentration (M L^{-3})
C_0	volume-averaged input concentration (M L^{-3})
C_p	peak tracer concentration (M L^{-3})
d_i	data value derivatives
D_z	axial dispersion (L^2 T^{-1})
$f(x^*)$	function representing the real root of the ADE
g_i	input concentrations for pulse injection; (i=1,2; g_0=g_2=0)
$g(t)$	function of values such that $g(t_i)$=C_i
$\hbar$	Hermite cubic basis function
$\hat{\hbar}$	Hermite cubic basis function
H	solute-migration zone thickness (L)
I	integrand of a function
I'	approximate integrand of a function
$\bar{\gamma}_i$	upper bounds on $\mathbf{y}$
$\underline{\gamma}_i$	lower bounds on $\mathbf{y}$
Γ_i^E	auxiliary functions for equilibrium transport [Table 1; (i=1,2,3)]
k	CSTR reaction rate constant (T^{-1})
K_a	fracture and/or solution conduit distribution coefficient (L)
K_d	solute distribution coefficient (L^3 M^{-1})
L	characteristic distance from point of injection to point of recovery (L)
M	tracer mass (M)
M_B	dimensionless mass of applied tracer for a Dirac input $= \frac{M/A}{c_0 L}$
n	number of evaluation points (dimen.)
n_b	number of additional samples to be collected prior to expected tracer breakthrough
n_e	effective porosity (dimen.)
n_κ	number of evaluation points for Chatwin analysis (dimen.)
n_m	multiplier for estimating tracer-test duration (dimen.)
n_s	number of samples to be collected
θ	porosity (dimen.)
$\mathbf{p}$	components M, R_d, and μ of vector $\mathbf{y}$ to be optimized
P_e	Péclet number $= \frac{vL}{D_z}$ (dimen.)
ρ_b	bulk density (M L^{-1})
q	inflow into injection point at time of injection (L^3 T^{-1})
Q	flow system discharge (L^3 T^{-1})
r	conduit radius (L)
$\hat{r}$	$_i(y)$twice continuously differentiable functions of y
R_d	solute retardation (dimen.)
σ_t^2	travel time variance (T^2)
t	time (T)
$\bar{t}$	average time of travel (T)
t_b	base time value for Δt time spacing (T)
t_d	tracer-test duration corresponding to last detectable tracer breakthrough (T)
t_κ	maximum allowable time for Chatwin analysis $t_\kappa \leq \frac{z}{v}$ (T)
t_m	base time value for $n_m \Delta t$ time spacing (T)
t_0	time for pulse release (T)
t_p	expected time to peak arrival (h)
t_R	tracer release control (dimen.)
t_s	sample-collection times (T)
t_{sf}	sampling frequency (T)
t_{sm}	time corresponding to minimum concentration for sample collection (T)
Δt	time spacing for CSTR-generated BTC (T)
T	dimensionless time $= \frac{vt}{L}$

$\bar{T}$ dimensionless mean residence time $= \frac{\upsilon \bar{t}}{L}$
$\hat{T}_i$ dimensionless pulse time $= \frac{\upsilon t_0}{L}$; (i=1,2; $\hat{T}_1$=0)
μ solute decay (T^{-1})
μ^E dimensionless equilibrium decay $= \frac{L(n_e\mu_l+\rho_b K_d\mu_s)}{n_e\upsilon}$; $\frac{L(b\mu_l+2K_a\mu_s)}{b\upsilon}$; $\frac{L(r\mu_l+2K_a\mu_s)}{r\upsilon}$
μ_l liquid phase solute decay (T^{-1})
μ_s sorbed phase solute decay (T^{-1})
υ mean tracer velocity ($L\ T^{-1}$)
$\bar{\upsilon}$ mean tracer velocity for the CSTR-generated BTC ($L\ T^{-1}$)
V flow system volume (L^3)
W width of solute-migration zone (L)
$\mathbf{x}$ vector of straight-line parameters used in the Chatwin analysis ($T^{1/2}$)
$\mathbf{y}$ vector of p components (M, R_d, and μ) to be optimized
z distance (L)
Z dimensionless distance $= \frac{z}{L}$

References

Barth GR, Illangasekare TH, Hill MC, Rajaram H (2001) A new tracer-density criterion for heterogeneous porous media. Water Resour Res 37(1):21–31

Chatwin PC (1971) On the interpretation of some longitudinal dispersion experiments. J Fluid Mech 48(4):689–702

Dennis JE, Gay DM, Welsch RE (1981) An adaptive nonlinear least-squares algorithm. ACM Trans Math Softw 7(3):348–383

Field MS (1997) Risk assessment methodology for karst aquifers, 2, solute-transport modeling. Environ Monit Assess 47:23–37

Field MS (2002) Efficient hydrologic tracer-test design for tracer-mass estimation and sample-collection frequency. 2. Experimental results. Environ Geol (in press). DOI 10.1007/s00254-002-0592-1

Field MS, Pinsky PF (2000) A two-region nonequilibrium model for solute transport in solution conduits in karstic aquifers. J Contam Hydrol 44:329–351

Field MS, Wilhelm RG, Quinlan JF, Aley TJ (1995) An assessment of the potential adverse properties of fluorescent tracer dyes for groundwater tracing. Environ Monit Assess 38:75–96

Freeze RA, Cherry JA (1979) Groundwater. Prentice-Hall, Englewood Cliffs

Kahaner DK, Moler C, Nash SG (1989) Numerical Methods and software. Prentice-Hall, Englewood Cliffs

Käss W (1998) Tracing technique in geohydrology. Balkema, Rotterdam

Kilpatrick FA, Wilson JF Jr (1989) Measurement of time of travel in streams by dye tracing. Techniques of water-resources investigations of the US Geological Survey, Book 3, Chapter A9, Washington, DC

Levenspiel O (1999) Chemical reaction engineering. Wiley, New York

Małoszewski P, Harum T, Benischke R (1992) Mathematical modelling of tracer experiments in the karst of Lurbach system. In: H Behrens, R Benischke, M Bricelj, T Harum, W Käss, G Kosi, HP Leditzky, C Leibundgut, P Maoszewski, V Maurin, V Rajner, D Rank, B Reichert, H Stadler, W Stichler, P Trimborn, H Zojer, M Zupan (eds) Investigations with natural and artificial tracers in the karst aquifer of the Lurbach system (Peggau–Tanneben–Semriach, Austria). Steirische Beiträge zur Hydrogeologie, 6th International Symposium on Water Tracing, Transport Phenomena in Different Aquifers (Investigations 1987–1992), vol 43, pp 116–136, Joanneum Research, Graz, Germany

Novakowski KS (1992) The analysis of tracer experiments conducted in divergent radial flow fields. Water Resour Res 28(12):3215–3225

Oostrom M, Hayworth JS, Dane JH, Güven O (1992) Behavior of dense aqueous phase leachate plumes in homogenous porous media. Water Resour Res 28(8):2123–2134

Parriaux A, Liskay M, Müller I, della Valle G (1988) Guide pratique pour l'usage des traceurs artificiels en hydrogéologie. Société Géologique Suisse, Groupe des Hydrogéologues, GEOLEP EPFL, Lausanne, Switzerland

Silebi CA, Schiesser WE (1992) Dynamic modeling of transport process systems. Academic Press, San Diego

Smart CC (1988) Artificial tracer techniques for the determination of the structure of conduit aquifers. Ground Water 26(4):445–453

Sweeting MM (1973) Karst landforms. Columbia University Press, New York

Toride N, Leij FJ, van Genuchten MT (1993) A comprehensive set of analytical solutions for nonequilibrium solute transport with first-order decay and zero-order production. Water Resour Res 29(7):2167–2182

Toride N, Leij FJ, van Genuchten MT (1995) The CXTFIT code for estimating transport parameters from the laboratory or field tracer experiments; version 2.0. Tech Rep 137, US Salinity Lab, Riverside, California

Webster DS, Proctor JF, Marine IW (1970) Two-well tracer test in fractured crystalline rock. US Geological Survey Water-Supply Paper 1544-I, Washington, DC

Wolff HJ, Radeke KH, Gelbin D (1979) Heat and mass transfer in packed beds. iv: Use of weighted moments to determine axial dispersion coefficients. Chem Eng Sci 34:101–107

Yevjevich V (1972) Stochastic processes in hydrology. Water Resources Publications, Fort Collins